Journal of Materials Chemistry A

Soft double-network polydimethylsiloxane: Fast healing of fracture toughness

Journal:	*Journal of Materials Chemistry A*
Manuscript ID	TA-ART-02-2022-000887.R1
Article Type:	Paper
Date Submitted by the Author:	22-Apr-2022
Complete List of Authors:	Chen, Chao; University of Massachusetts Amherst, Polymer Science and Engineering Fei, Huafeng; Institute of Chemistry, Chinese Academy of Sciences, Watkins, James; University of Massachusetts Amherst, Polymer Science and Engineering Crosby, Alfred; University of Massachusetts, Polymer Science and Engineering

Soft double-network polydimethylsiloxane: Fast healing of fracture toughness

Chao Chen,[1†] *Hua-Feng Fei*, [1†] *James J. Watkins*, [1*] *Alfred J. Crosby*[1*]

Department of Polymer Science and Engineering, University of Massachusetts Amherst, Amherst, Massachusetts 01003, United States.

† Both authors contribute equally.

* AJC: acrosby@umass.edu, JJW: watkins@polysci.umass.edu.

Keywords: Double-network polydimethylsiloxane; Fast self-healing; Tough and soft

ABSTRACT

Solvent-swollen double-network materials containing one dynamic network and one permanent network offer softness, toughness, and fast-healing functionality. However, achieving these multiple functionalities in solvent-free materials remains a challenge. Herein, we develop a soft, solvent-free, double-network polydimethylsiloxane (DN-PDMS) material. A covalent bottlebrush network with low crosslink/entanglement densities provides ultralow stiffness. A dynamic borate network dissipates energy to toughen the material and self-heals to recover toughness from damages/pre-cuts. The high mobility of bottlebrush architecture and fast bond-reforming kinetics of borate network provide fast self-healing without stimuli. A DN-PDMS with an equal weight of each network demonstrates a fracture toughness of 3.8 kJ/m^2 and a failure strain of 15. When cut materials are brought into contact for 10 seconds, the material recovers to a toughness of 1.5 kJ/m^2 and a failure strain of 7. The fast-healing DN-PDMS with softness and toughness offers a significant advance by providing toughness and healing without a solvent.

1. INTRODUCTION

Polydimethylsiloxane (PDMS) is a solvent-free silicone material [1] with high thermal and electric resistance, low-temperature elasticity, hydrophobicity, and biocompatibility [2]. It works in extreme conditions, such as high or low temperatures, high radiation, and low humidity, and widely serves in sealants [3–5], cookwares, dielectric elastomers [6], soft electronics [7,8], microfluidics [9,10], and biomaterials [2]. Recently, PDMS materials have been made ultrasoft with bottlebrush architecture of reduced polymer chain entanglements [11–16]. However, these ultrasoft bottlebrush PDMS networks typically suffer from brittleness and lack healing capability.

Achieving multiple performances, such as high toughness, ultra-low stiffness, and fast self-healing, in a solvent-free material is challenging. The traditional toughening approach of adding fillers of nanoparticles or fibers simultaneously increases the materials' moduli [17]. The strategy of using a double-network (DN) or an interpenetrating network structure can toughen materials and maintain softness [18–20]. For double-network materials swollen with solvents, additional fast healing functionality is gained by incorporating self-healing dynamic networks [21–28]. However, achieving such a combined performance in solvent-free materials remains a challenge (Table 1), limited by the immiscibility between networks without a cosolvent [29–32].

Over the past decade, with the emergence of various dynamic solvent-free networks, such as vitrimers [33] and covalent adaptable networks [34], some have demonstrated fast healing performance. In particular, the borosiloxane-based materials have long been used for Silly Putty toys [35,36] and recently have been studied intensively for fast self-healing, energy absorbent polymeric materials. For example, Lai et al. [37] developed a boroxine elastomer that self-heals its stiff network in seconds assisted with moisture, and a dynamic borate PDMS network that heals in 10 minutes has demonstrated excellent impact energy absorption and buffering [38]. However,

these materials contain only dynamic networks and lack the resilience and strength to serve as load-bearing materials. Double-network materials, which usually contain at least one covalent network, are ideal candidates for soft structural materials. Incorporating a dynamic self-healing network into a solvent-free DN silicone material improves its load-bearing and self-healing performance [39]. Typically, healing of mechanical performance takes tens of minutes or longer [40–43] (Table 1), limiting the mechanical applications with repeated loads.

Table 1. Mechanical performances of various solvent-free double-network materials.

Source	Dynamic Unit	Toughness (J/m^2)	Stretchability	Healing Time	Modulus (kPa)
J. L. Self, et al. [43]	Ester	–	3.50	5 h (180 °C)	Shear, 10–100
L.-H. Cai, et al. [12]	–	–	1.44 [44]	–	Shear, 7–132
W. F. M. Daniel, et al. [13]	–	–	–	–	Shear, 0.1–12
J. Kang, et al. [41]	Hydrogen bond	12000	12	48 h (R.T.)	Tensile, 400–500
Z. Wang, et al. [45]	–	300–12000	18.5	–	Tensile, 400–1600
This work	Borate bond	3800	15	10 s (R.T.)	Tensile, 50–200

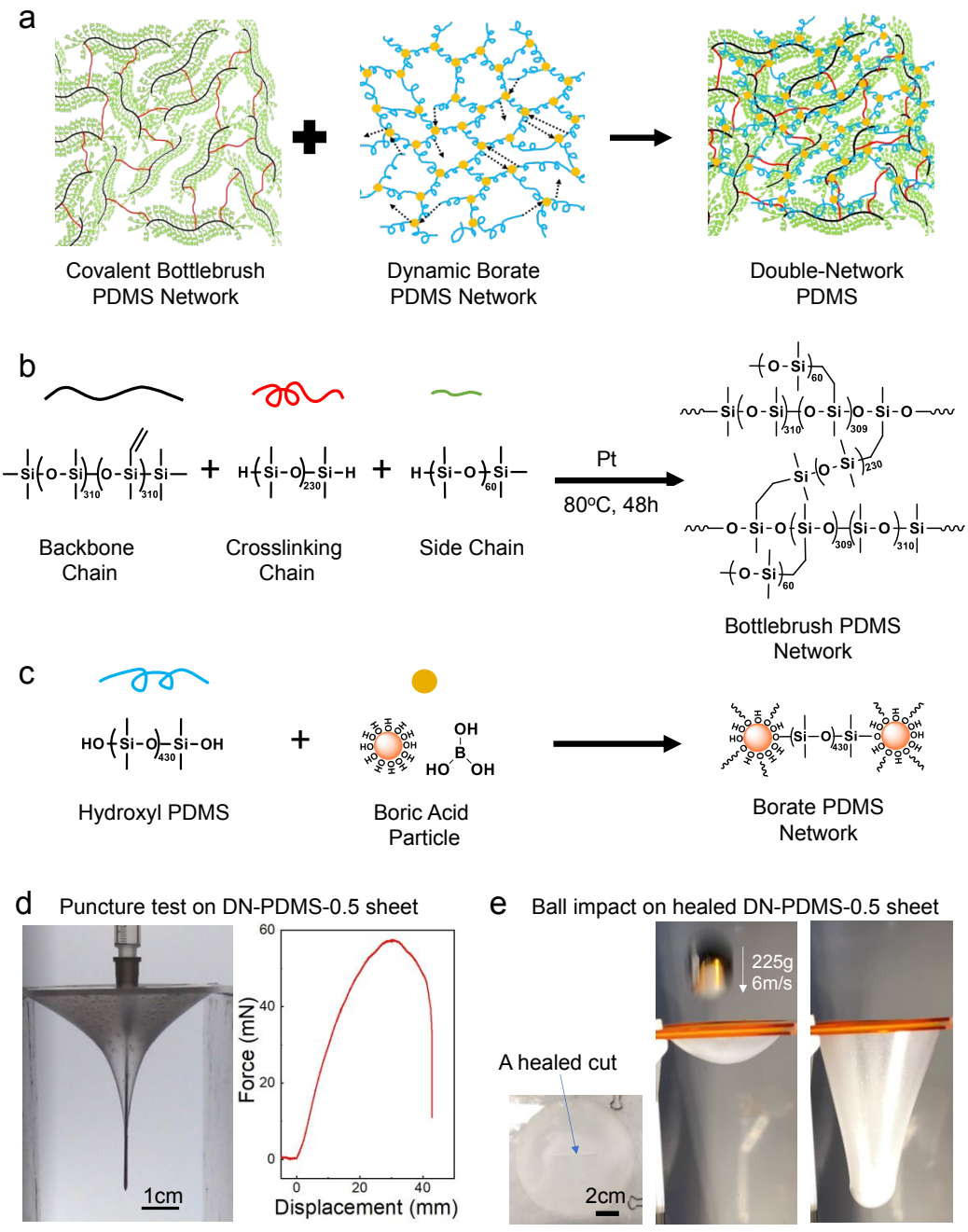

Figure 1. (a) A DN-PDMS is comprised of two independent and interpenetrating PDMS networks: a covalent bottlebrush network and a dynamic borate network. (b) The covalent bottlebrush PDMS is synthesized through a hydrosilylation reaction. The side chains are grafted to the backbone chains to form bottlebrush strands, and crosslinking chains connect the strands to form a network. (c) The dynamic PDMS network is synthesized through a reversible siloxane condensation reaction between hydroxy-terminated PDMS chains and boric acid particles. (d) Puncture test on a sheet of DN-PDMS-0.5. The sheet has a thickness of 1.6 mm and a diameter of 45 mm. The indenter is a beveled medical needle with a diameter of 0.7 mm. The force–displacement response of the deep indentation to rupture with an indentation velocity of 0.2 mm/s. (e) Impact tests on a

cut and healed sheet of DN-PDMS-0.5. A circular membrane with a thickness of 3 mm and a diameter of 100 mm was cut in the center and allowed to heal for 30 seconds in ambient condition. The circumference was clamped. A 225-gram steel ball dropped from a height of two meters and impacted the film at a speed of ~ 6 m/s. The membrane broke at the seventh successive impact and showed good elasticity and shape recovery before the failure.

Despite the above-mentioned advances, achieving the multiple functionalities of softness, toughness, and fast self-healing in a solvent-free material remains a challenge. In this work, we develop a soft double-network polydimethylsiloxane (DN-PDMS) that can heal to recover the fracture toughness in as little time as 10 seconds. The DN-PDMS is comprised of two miscible PDMS networks: a covalently crosslinked bottlebrush PDMS network and a dynamic borate PDMS network (Figure 1a–1c). The bottlebrush covalent network has a low density of crosslinks and entanglements to reduce stiffness. The dynamic borate PDMS network is dissipative to toughen material, while also providing a mechanism for self-healing. The fast healing rate is attributed to the high mobility of bottlebrush architecture and fast bond-reforming of borate network. We demonstrate a DN-PDMS with equal weight of the comprised networks with a fracture toughness of 3.8 kJ/m^2, a failure strain of 13.9, flaw-insensitivity to a centimeter-long notch, and a high puncture resistance to a beveled medical needle as demonstrated in Figure 1d. When cut and placed back in contact for 10 seconds, the material recovers the DN-PDMS to a toughness of over 1.5 kJ/m^2 and a failure strain of 7. The cut and healed DN-PDMS can survive in repeated successive impacts in Figure 1e (Movie 1 in SI). We anticipate that the fast healing PDMS with ultra-fast bond reforming kinetics will guide the design of soft and tough materials that can bear repeated mechanical loads.

2. MATERIAL SYNTHESIS

We carried out a one-step procedure to synthesize the double-network PDMS in a solvent-free environment. We adopted the procedure of Cai et al. [12] to form the bottlebrush PDMS. Multi-functional trimethylsiloxy-terminated linear vinylmethylsiloxane-dimethylsiloxane serves as the backbone. Monohydride-terminated linear PDMS was grafted to the backbone as side chains. Dihydride-terminated linear PDMS served as covalent crosslinking chains to bridge the grafted bottlebrush strands to form a covalent network. The hydrosilylation reaction requires a platinum catalyst at 80 ^{o}C for 48 hours (Figure 1b). We used the condensation reaction between the hydroxy-terminated PDMS and boric acid microparticles [38] to form a dynamic borate PDMS network (Figure 1c). These distinct reactions allow for a double-network structure with two independent and interpenetrating networks (Figure S1). After blending all ingredients, the polymer formulation was degassed and poured into an open mold in a dry, 80 ^{o}C nitrogen atmosphere for 48 hours to cure. The double-network PDMS sample was kept in the dry nitrogen atmosphere at room temperature before use. The ratio between the bottlebrush PDMS and the dynamic PDMS is adjustable. We denote the resultant as **DN-PDMS-*x***, where *x* indicates the weight fraction of the dynamic borate PDMS network. All the materials are commercially available and affordable for batch sample preparation. The material shows light scattering by residual boric acid particles in the submicron size, which leads to the opaque white color (Figure S2). Meanwhile, the small-angle X-ray scattering confirms that no structural phase separation occurs on nanometer length scales (Figure S3). The similar chemistry of the PDMS chains allows for these two networks' miscibility, providing a general approach to developing homogeneous DN materials without a cosolvent.

3. TOUGH AND SOFT DOUBLE-NETWORK PDMS

We characterized the mechanical performance of the DN-PDMS through pure-shear tensile and fracture tests shown in Figure 2a. We used the DN-PDMS-0.5 as a focused case with the equal weight of the two PDMS networks. We clamped a rectangular sample to a width of 30 mm, a thickness of ~ 3 mm, and a height of ~ 10 mm. We pulled the sample uniaxially to failure. Except where indicated, we conducted all tests at room-temperature (20 ^{o}C – 25 ^{o}C) in a dry-nitrogen (relative humidity (RH) ~ 16%) atmosphere, and we fixed the strain rate to 0.02 per second. Without an edge cut, a DN-PDMS-0.5 material can be stretched up to a strain of 15 before breaking. With a one-centimeter-long edge cut, the strain at break remains 14 (Figure 2a). The highly flaw-insensitive fracture behavior is distinct from brittle materials and consistent with many tough hydrogels and bio-tissues [46].

The stress–strain curves in the tensile tests in Figure 2b show that the double-network PDMS exhibits enhanced stretchability and reaches greater levels of stress compared to individual networks. Without the double-network structure, the single covalent bottlebrush network breaks at a strain of 0.97, and the single dynamic borate PDMS yields and flows when the applied strain reaches 0.22, attributed to the borate bond's dynamic nature. With the double-network structure, the DN-PDMS yields at a strain around 1, stiffens until the stress reaches its peak around a strain of 8, and gradually fails. The pure-shear tensile response can be divided into three regimes (Figure 2b and Figure S4): the low strain regime before yielding (regime 1), the intermediate strain regime between the yielding point and the peak stress (regime 2), and the high strain regime where the stress degrades (regime 3). Regime 1 corresponds to a small elastic deformation of the original networks. In regime 2, the dynamic bond network starts to incur damage and dissipate strain energy, and the covalent bonds maintain the network's integrity and elasticity. In regime 3, the covalent

bottlebrush network sustains severe damage, evidenced by the significant decrease in loading stress.

We measured the fracture energy for the samples with different weight ratios of the two networks (Figure 2c). The DN-PDMS-0.5 reaches the highest fracture energy of 3.8 kJ/m^2, 75 times larger than that of the pure PDMS bottlebrush network (50 J/m^2). Note that the fracture energy was obtained with the sample height of ~ 10 mm. A larger fracture energy is anticipated for larger DN-PDMS samples [46,47].

The toughness is also reflected in the high puncture resistance, as shown in the beveled medical needle puncturing a DN-PDMS-0.5 sheet (Figure 1d). The sheet has a thickness of 1.6 mm and a diameter of 45 mm, and the needle was inserted at a velocity of 0.2 mm/s. The membrane breaks when the indentation depth reaches 43 mm.

To measure the softness of the materials at low applied strain, we performed dynamic mechanical analysis (DMA) tests (Figure 2d). We fixed the strain oscillation with a low frequency of 0.1 Hz and a small strain amplitude of 0.01. We set the humidity to zero and the temperature to 25 ^{o}C in the DMA's environmental chamber. The storage moduli fall between 10 kPa to 200 kPa with various weight ratios. The low-modulus PDMS is softer than most solvent-free elastomers without bottlebrush structures [45] and is comparable to many hydrogels [48] and tissues [49]. The moduli follow a nearly linear trend with the weight percentage of the comprised networks, allowing for straightforward programming of the stiffness by controlling the weight ratio of the two networks. The linear relationship between the storage moduli and the weight fraction of linear PDMS chains in Figure 2d suggests that adding linear chains to dilute the bottlebrush network does not have a significant influence on the crosslinking process. We include a diagram of the fracture energy versus the mechanical modulus for various solvent-free rubbery materials in Figure

2e [45]. The DN-PDMS is softer than many solvent-free elastomers and is tougher than pure bottlebrush PDMS materials.

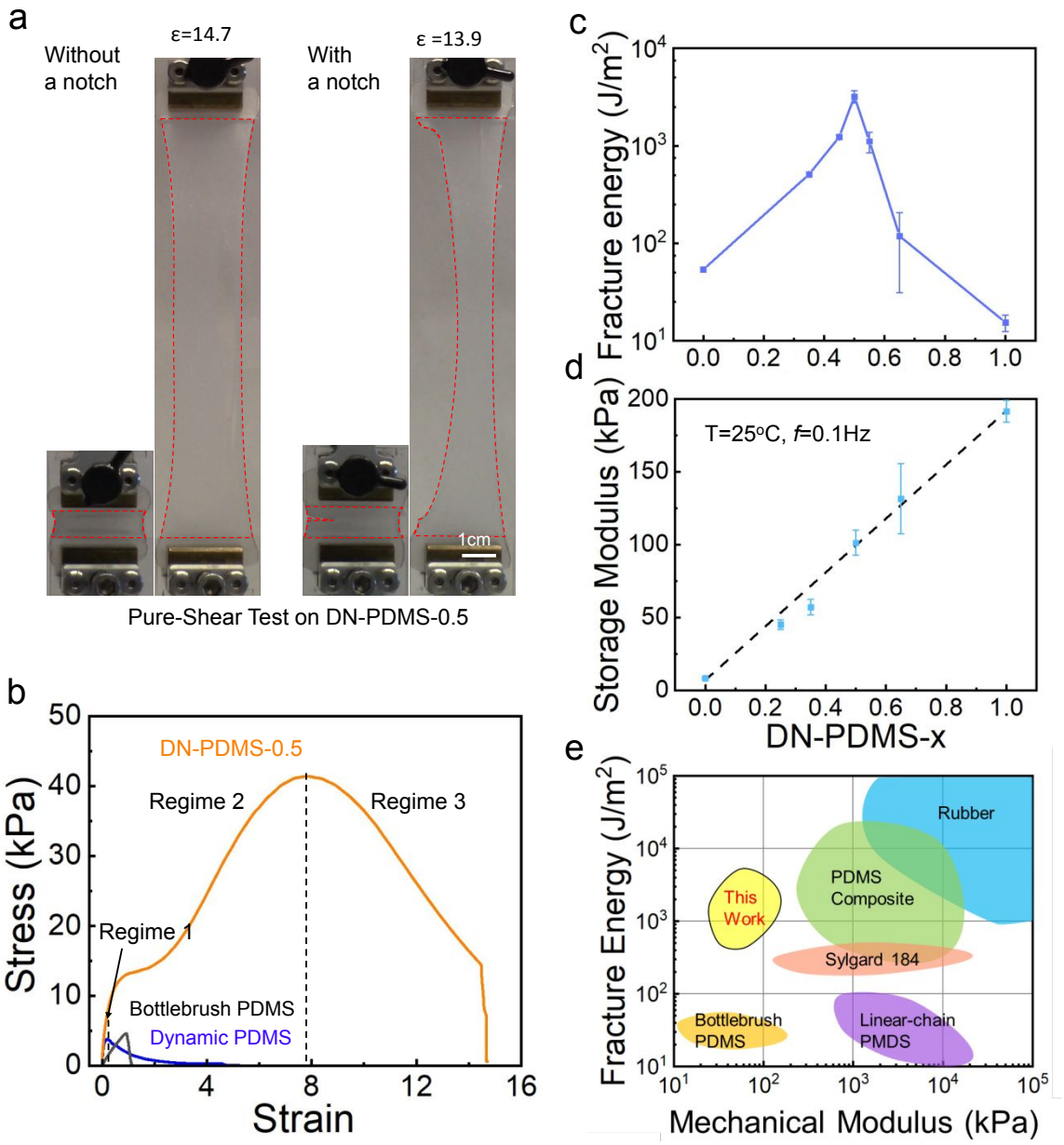

Figure 2. A stretchable, tough, and soft PDMS material. (a) Pure-shear tests on the DP-PDMS-0.5 samples without a notch and with a one-centimeter-long edge notch. The sample's width before stretching is 30 mm, the height ~ 10 mm, and the thickness ~ 3 mm. (b) The stress–strain responses of the DN-PDMS, the bottlebrush PDMS, and the borate PDMS. (c) The fracture energy of the DN-PDMS with various weight percentages of dynamic borate network, *x*. The measurement was taken at 20 °C – 25 °C, a relative humidity of 16 %, and a strain rate of ~ 0.02 s^{-1}. (d) Storage moduli of DN-PDMS-*x* through dynamic mechanical analysis. The dashed line shows a linear guideline. The oscillation strain amplitude is 1 %. The relative humidity is zero. (e) A diagram of the fracture energy and the mechanical modulus for various solvent-free rubbery materials.

While the above-mentioned mechanical properties were measured under slow loading rates (0.02 s^{-1} in the pure-shear tests and 0.1 Hz in the DMA tests), the stress–strain responses (Figure S5a) and fracture toughness (Figure S5b) vary with loading rate due to the contribution of the dynamic network. However, this dynamic nature also opens an avenue for fast healing of the DN materials. In the following section, we describe DMA measurements to investigate the dynamic rheological response and the associated timescale that governs the healing behavior.

4. RATE-DEPENDENT RHEOLOGY OF DN-PDMS

We use DMA to characterize the rate-dependent rheological behaviors of the DN-PDMS networks. Figure 3 shows the rheological responses measured over a broad frequency range from 10^{-3} Hz to 10^{2} Hz at room temperature (~ 25 ^{o}C) and zero humidity. Additional data are shown in Figure S6–S8. Figure 3a includes the storage and loss moduli and the phase angle of DN-PDMS-0.5. When the frequency is higher than 0.05 Hz, the DN-PDMS-0.5 exhibits a rubbery plateau with a storage modulus of ~100 kPa, which is significantly higher than the loss modulus. When the frequency is lower than 0.01 Hz, the storage moduli monotonically decrease to less than the loss moduli, showing fluid-like properties at low frequencies.

Figure 3b compares the storage moduli of the DN-PDMS-0.5, the dynamic PDMS, and the bottlebrush PDMS. The low-frequency data are power-law extrapolations as denoted as dashes. In comparison, the linear superposition of the constituents' rheological behaviors is indicated by the red curve. The DN-PDMS-0.5 matches the linear superposition at the high-frequency rubbery state but deviates significantly at the low-frequency range, suggesting that the dynamic and bottlebrush networks couple in a nonlinear manner to control the dynamics of the double network material.

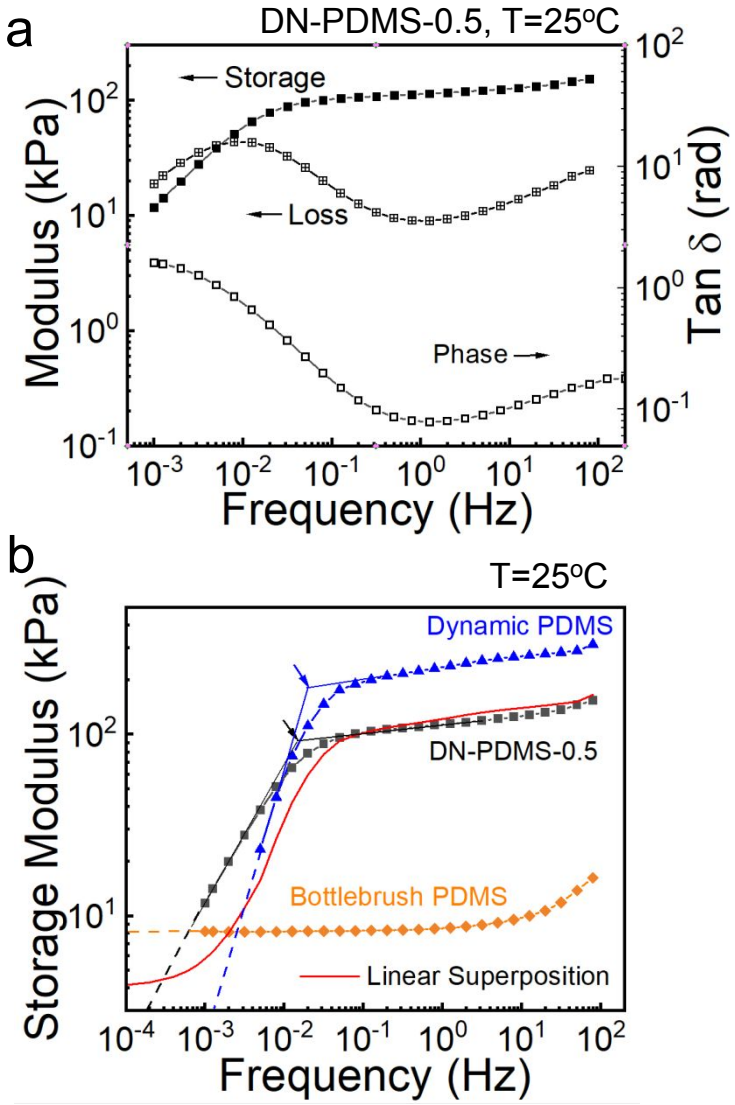

Figure 3. Rheology of the double-network PDMS materials and individual networks. (a) Frequency dependence of the storage and loss moduli and phase angles of DN-PDMS-0.5 at 25 °C and zero humidity. (b) Frequency dependence of the storage moduli of DN-PDMS-0.5 and the comprising networks at 25 °C. The red curve shows the storage moduli through the linear superposition between the dynamic PDMS and the bottlebrush PDMS. Dashes are power-law extrapolations at the low-frequency regime. Arrows indicate the transition from the rubbery state to the fluid-like state.

The timescale of the rheological change is also included in Figure 3. The timescale of the rheological change related to the bond reforming processes was investigated by Cai, et al. [12] and Zhu, et al. [50]. For our material system, the transition frequency 0.022 Hz of the pure dynamic PDMS, marked as a blue arrow in Figure 3b, corresponds to the characteristic timescale of $\tau = 45$

s of the dynamic network's reforming. The transition frequency 0.016 Hz of the DN-PDMS-0.5, marked as a black arrow in Figure 3b, corresponds to the characteristic timescale of $\tau = 63$ s, which is consistent with the significant decrease in the phase angle (Figure 3a). The increase of τ from 45 s for the dynamic PDMS to 63s for the DN-PDMS-0.5 reflects the change of the bond reforming rates.

This deviation in the timescale indicates that in the dual-network system the dynamic physical interactions governing healing rates are not restricted to the borate network. The hydroxy-terminated linear-chain PDMS can also form physical entanglements and hydrogen bonds with the bottlebrush structures [41]. In particular, the unique bottlebrush architecture with dense sidechains may play an advantageous role in increasing the interaction with other networks. The fast kinetics of bond reforming not only imparts the strong rate-dependent mechanical responses but also enables desired fast healing and recovery behaviors, as we discuss in the following section.

5. FAST RECOVERY AND HEALING

We evaluate two performance metrics related to the self-healing ability of the material. One is the recovery of the stress-strain response from a preceding loading cycle. The internal damage caused by the initial loading history will reduce the stress level in a subsequent loading cycle for a non-self-healing material. A self-healing material can reform damaged bonds and restore the stress-strain response. The other healing performance is the restored strength of an interface formed by contacting two surfaces formed through a previous cut. We discuss both performances. To distinguish them in this work, we call the former behavior *recovery* and the latter one *healing*.

5.1 Fast recovery from preceding loading

The double-network material loses its toughness after the first loading when the broken sacrificial bonds experience no bond reformation. By incorporating the self-healing dynamic bonds, the double-network materials regain their double-network structure and toughness over time [19,20]. The recovery time of the dynamic networks limits the achievable toughness between consequent loads. We examine the recovery of the mechanical performance from a previous loading cycle through the pure-shear tensile test, with a sample stretched to a strain of 0.5 (Figure 4a,b) and 1.0 (Figure 4c,d) and unloaded to the initial dimension. The sample rested for a prescribed time and then was re-stretched to the same maximum strain.

Figures 4a and 4b show the fast recovery of the stress–strain response after the DN-PDMS-0.5 samples are unloaded from a preceding strain of 0.5. With 15 s of dwelling during which the sample is static, the sample recovers 77% of the initial strain energy, and with 30 s of dwelling, 80% of the strain energy is recovered. A 2-minute dwelling leads to almost full recovery of the initial stress–strain response, and the strain energy recovers 96%.

Figures 4c and 4d include the recovery of the stress–strain response after the DN-PDMS-0.5 samples are unloaded from a larger strain of 1.0. The 15s-dwelling recovers 66% of the initial strain energy density. After 30 minutes of dwelling, the recovered strain energy increases to 83%, but the stress–strain response still deviates from the response measured during the initial loading cycle noticeably. The more limited partial recovery for cycles with larger maximum strain is attributed to damage in the covalent bottlebrush networks.

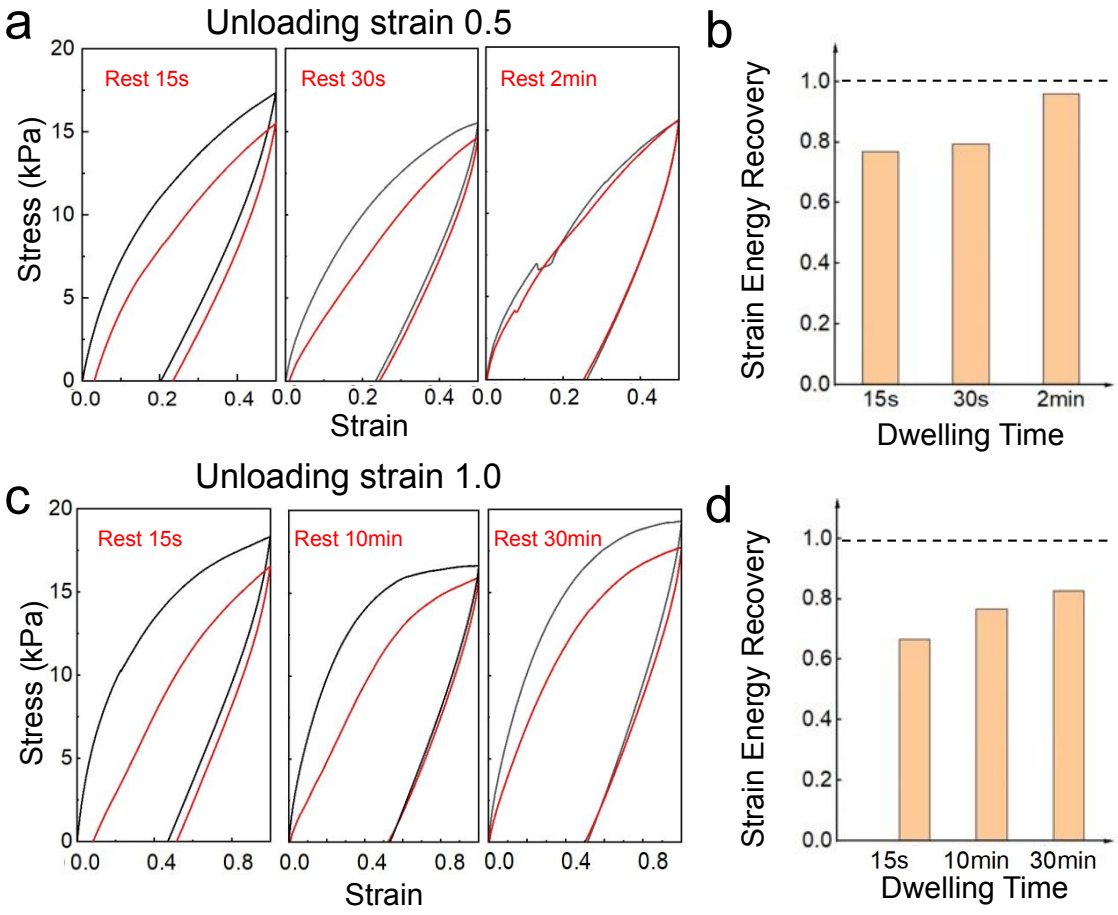

Figure 4. Mechanical recovery from a preceding stretch with an unloading strain of (a,b) 0.5 and (c,d) 1.0. (a,c) A pure-shear sample for the first loading and the subsequent reloading with various resting time. The black curves represent the first loading and unloading responses. The red curves represent the second loading and unloading responses. (b,d) The strain energy recovery compared to the first load.

While the recovery of strain energy at moderate timescales is advantageous for healing during cyclic loading, the dissipation of energy at faster timescales can slow fracture propagation. The hysteretic loading and unloading loops in Figures 4a and 4c demonstrate over 80% of the strain energy is dissipated over the cycles. We include the dissipative behavior under various unloading strain in Figure S9 in the SI. After the applied recovery time of 30 s, the second loading and unloading loop still shows a large hysteretic dissipation, indicating that the materials remain

tough after the recovery of the sacrificial network. For future studies, more sophisticated characterizations, such as the continuous oscillation step strain experiments, would be interesting to provide additional characterization and insights into recovery processes.

We directly examine the resistance to crack growth for the double-network PDMS under prolonged cyclic loading in Figure S10. We cut a DN-PDMS-0.5 sample from the edge to introduce an initial edge crack with a length of 1 cm. We then stretched the pure-shear sample to a prescribed strain and unloaded the sample to its original height. Under a slow cyclic load with a period of 30 s, the edge crack does not grow over 11,000 cycles with an applied maximum strain of 1. We also demonstrate that under a slower cyclic load with a period of 60 s, the edge crack length remains unchanged with a higher strain of 2.0. In contrast, when the DN-PDMS-0.5 experiences a higher frequency loading with a period of 1 s, the crack grows noticeably over 150,000 cycles. The distinct fatigue behaviors are in a similar time scale with the previous dynamic mechanical analysis that revealed a characteristic timescale of 63 s. When the cyclic period is much larger than the material's characteristic timescale, the DN-PDMS recovers its mechanical performance to resist crack growth in the following cycle. When the cyclic period approaches or becomes shorter than the characteristic timescale, the recovery is insufficient to resist fatigue. This finding provides a perspective to the design of anti-fatigue double-network materials [51] by incorporating self-healing sacrificial networks whose healing is faster than the loading frequency.

5.2 Fast healing from a cut

The DN-PDMS demonstrates fast healing after the material is cut and put back in contact for a certain dwelling time before load. We define the healing time as the dwelling time before load. We pulled the healed sample to failure to characterize the mechanical performance after healing (Figure 5a). Manually pulling a sample with a dwelling time of 10 seconds leads to a failure

strain of ~ 6.5 (Movie 2 in SI). With healing times of 30 s and one hour, Figure 5b shows the stress–strain responses of the healed samples. With a dwelling time of 30 seconds, the cut sample achieves a failure strain of 7 (Movie 3 in SI), nearly matching half of that of a non-cut material, and fracture energy of 1.5 kJ/m^2. Meanwhile, prolonged healing for one hour recovers to a failure strain of ~ 10 and fracture energy of ~ 2.9 kJ/m^2. As a comparison, the uncut sample's failure strain is 15, and the fracture energy is 3.8 kJ/m^2 (Figure 5b,c). The toughness value is comparable to several versions of tough hydrogels; however, the material introduced here does not require a volatile solvent to enhance mobility.

The toughness after healing is attributed to physical interactions between networks. The DN-PDMS is composed of two distinctive chemical bonds: the covalent siloxane bond and the dynamic B–O–Si bond. Introducing a cut in the DN-PDMS breaks both healable dynamic B–O–Si bonds and covalent siloxane bonds. In Figure 5d, we hypothesize that two mechanisms contribute to the healing performance of cut samples. (i) First, the B–O–Si network heals quickly after the cut. (ii) Additionally, when the covalent siloxane network is damaged, the broken chain-ends include reactive free radicals, which can form new borate networks with excess boric acid particles. The boron atoms bridge the damaged networks to reform the cut covalent networks' connectivity across the damage interface, which contributes to the toughness of the healed materials.

A significant benefit that the fast healing performance offers is the ability to reuse heavily damaged components (Figure S11). A previously torn sample was placed into a mold under heat and pressure for 24 hours to reform the pure-shear geometry. The remolded specimen still shows a failure strain of 6 before rupture. As the preceding loading had mostly broken the covalent network in the DN-PDMS, the residual covalent network and the dynamic interactions between the bottlebrush network and the linear chain network still construct a double-network structure that

toughens the material. These remoldable and recyclable dynamic polymers attributes are exciting for eco-friendly material management[52–54].

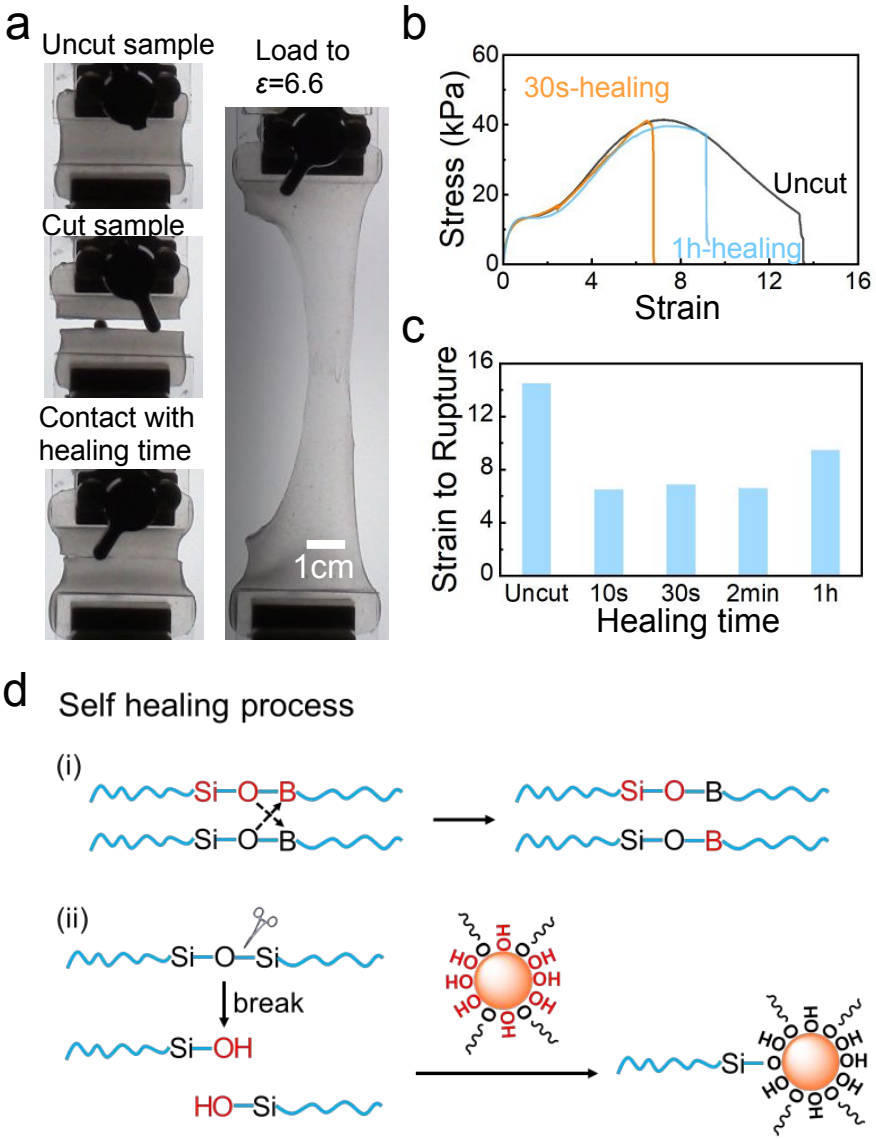

Figure 5. Fast healing of DN-PDMS-0.5 from a cut. (a) Pure-shear stretching test on a healed sample. A pure-shear sample is cut into two pieces and brought to contact for 30 seconds. The sample is stretched by a texture analyzer to rupture. (b) The stress–strain responses of a healed sample with 30 s contact time and an intact sample. (c) The stretchability of the uncut sample and the healed samples with various dwelling time. (d) Schematics of the two pathways of reforming the dynamic B–O–Si network.

6. ENVIRONMENTAL SENSITIVITY

While the softness, toughness, and fast healing ability of the DN-PDMS system are attractive attributes, the borate network is sensitive to environmental conditions such as the temperature and moisture. As all previous tests were conducted at low relative humidity (RH = 16% in the pure-shear testing and RH = 0% in the DMA testing) and room temperature, the temperature (Figure S7) and humidity (Figure S8) dependences on the rheological behavior are provided in the SI. Not surprisingly, the properties of the covalently-bonded bottlebrush PDMS network are insensitive to the environment, but the storage moduli of the dynamic borate network decrease at higher levels of temperature and humidity. This decrease also leads to a decrease in the DN-PDMS materials. While this decrease could be detrimental for some applications, it could open up opportunities for applications that require responsiveness to environmental stimuli.

7. CONCLUSION

We have developed a soft and tough double-network PDMS material that can quickly self-heal to recover toughness. The similar chemistry of the comprised networks allows for the miscibility to form a homogeneous DN material without a cosolvent. The commercially available ingredients are attractive for the potential scalability of these material systems. The fast healing double-network PDMS combines toughness and softness significantly greater than other solvent-free elastomers. After the material is cut and brought back in contact for seconds, it recovers with the fracture toughness of 1.5 kJ/m^2 (40% of the initial toughness) and the ability to achieve the maximum strains of 7, nearly half of the initial failure strain. The key lesson gained is that the fast kinetics of physical interactions not only exist in the dynamic borate bonds but also include the

dynamic interactions between the hydroxyl-terminated linear-chain PDMS and the bottlebrush PDMS. The eco-friendly DN-PDMS provides reusability along with impressive mechanical performance attributes. This desirable combination of properties paves a new pathway to developing soft and tough materials that can bear repeated mechanical loads in soft devices.

MATERIALS AND METHODS

Materials and Methods are included in the Supporting Information.

AUTHOR CONTRIBUTIONS

Study conception: C.C.; Material design: H.-F.F.; Data collection: C.C, H.-F.F.; Material analysis: H.-F.F.; Mechanical analysis: C.C.; Interpretation of results: C.C, H.-F.F., A.J.C.; First draft preparation: C.C.; Critical revision: C.C, H.-F.F., A.J.C.; Project supervision: A.J.C., J.J.W. All authors reviewed the results and approved the final version of the manuscript.

ACKNOWLEDGEMENT

C.C and A.J.C gratefully acknowledge the funding from Human Frontier Science Program (HFSP, No. RGP0019/2017). H.-F.F. and J.J.W. gratefully acknowledge the funding from ARL (W911NF1920152) and NCMS (HQ00341520007).

CONFLICT OF INTEREST

The authors declare no conflict of interest.

REFERENCE

[1] P. Mazurek, S. Vudayagiri, A. L. Skov, *Chemical Society Reviews* **2019**, *48*, 1448.

[2] P. N. Carlsen, *Polydimethylsiloxane: Structure and Applications*, Nova Science Publishers, Incorporated, **2020**.

[3] R. Flitney, *Seals and Sealing Handbook (Sixth Edition)*, Butterworth-Heinemann, **2014**.

[4] Q. Liu, Z. Wang, Y. Lou, Z. Suo, *Extreme Mechanics Letters* **2014**, *1*, 54.

[5] Z. Wang, C. Chen, Q. Liu, Y. Lou, Z. Suo, *Journal of the Mechanics and Physics of Solids* **2017**, *99*, 289.

[6] R. Pelrine, R. Kornbluh, Q. Pei, J. Joseph, *Science* **2000**, *287*, 836.

[7] D.-Y. Khang, H. Jiang, Y. Huang, J. A. Rogers, *Science* **2006**, *311*, 208.

[8] J. A. Rogers, T. Someya, Y. Huang, *Science* **2010**, *327*, 1603.

[9] M. Coux, C. Clanet, D. Quéré, *Applied Physics Letters* **2017**, *110*, 251605.

[10] J. C. McDonald, G. M. Whitesides, *Accounts of Chemical Research* **2002**, *35*, 491.

[11] Z. Cao, J.-M. Y. Carrillo, S. S. Sheiko, A. V. Dobrynin, *Macromolecules* **2015**, *48*, 5006.

[12] L. Cai, T. E. Kodger, R. E. Guerra, A. F. Pegoraro, M. Rubinstein, D. A. Weitz, *Advanced Materials* **2015**, *27*, 5132.

[13] W. F. Daniel, J. Burdyńska, M. Vatankhah-Varnoosfaderani, K. Matyjaszewski, J. Paturej, M. Rubinstein, A. V. Dobrynin, S. S. Sheiko, *Nature Materials* **2016**, *15*, 183.

[14] M. Vatankhah-Varnoosfaderani, W. F. Daniel, A. P. Zhushma, Q. Li, B. J. Morgan, K. Matyjaszewski, D. P. Armstrong, R. J. Spontak, A. V. Dobrynin, S. S. Sheiko, *Advanced Materials* **2017**, *29*, 1604209.

[15] H. Liang, S. S. Sheiko, A. V. Dobrynin, *Macromolecules* **2018**, *51*, 638.

[16] S. S. Sheiko, A. V. Dobrynin, *Macromolecules* **2019**, *52*, 7531.

[17] A. S. Hashim, B. Azahari, Y. Ikeda, S. Kohjiya, *Rubber Chemistry and Technology* **1998**, *71*, 289.

[18] J. P. Gong, Y. Katsuyama, T. Kurokawa, Y. Osada, *Advanced Materials* **2003**, *15*, 1155.

[19] J.-Y. Sun, X. Zhao, W. R. Illeperuma, O. Chaudhuri, K. Oh, D. J. Mooney, J. J. Vlassak, Z. Suo, *Nature* **2012**, *489*, 133.

[20] C. Yang, M. Wang, H. Haider, J. Yang, J.-Y. Sun, Y. Chen, J. Zhou, Z. Suo, *ACS Applied Materials & Interfaces* **2013**, *5*, 10418.

[21] Y. Li, L. Yang, Y. Zeng, Y. Wu, Y. Wei, L. Tao, *Chemistry of Materials* **2019**, *31*, 5576.

[22] H. J. Zhang, T. L. Sun, A. K. Zhang, Y. Ikura, T. Nakajima, T. Nonoyama, T. Kurokawa, O. Ito, H. Ishitobi, J. P. Gong, *Advanced Materials* **2016**, *28*, 4884.

[23] Q. Zhang, M. Wu, X. Hu, W. Lu, M. Wang, T. Li, Y. Zhao, *Macromolecular Chemistry and Physics* **2020**, *221*, 1900320.

[24] D. Wei, J. Yang, L. Zhu, F. Chen, Z. Tang, G. Qin, Q. Chen, *Polymer Testing* **2018**, *69*, 167.

[25] S. Liu, L. Li, *ACS Applied Materials & Interfaces* **2017**, *9*, 26429.

[26] R. Long, K. Mayumi, C. Creton, T. Narita, C.-Y. Hui, *Journal of Rheology* **2015**, *59*, 643.

[27] W.-P. Chen, D.-Z. Hao, W.-J. Hao, X.-L. Guo, L. Jiang, *ACS Applied Materials & Interfaces* **2017**, *10*, 1258.

[28] X. Zhao, Y. Liang, Y. Huang, J. He, Y. Han, B. Guo, *Advanced Functional Materials* **2020**, *30*, 1910748.

[29] J. P. Gong, *Science* **2014**, *344*, 161.

[30] J. Wu, L. Cai, D. A. Weitz, *Advanced Materials* **2017**, *29*, 1702616.

[31] H.-F. Fei, W. Li, A. Bhardwaj, S. Nuguri, A. Ribbe, J. J. Watkins, *Journal of the American Chemical Society* **2019**, *141*, 17006.

[32] H.-F. Fei, B. M. Yavitt, X. Hu, G. Kopanati, A. Ribbe, J. J. Watkins, *Macromolecules* **2019**, *52*, 6449.

[33] D. Montarnal, M. Capelot, F. Tournilhac, L. Leibler, *Science* **2011**, *334*, 965.

[34] C. J. Kloxin, T. F. Scott, B. J. Adzima, C. N. Bowman, *Macromolecules* **2010**, *43*, 2643.

[35] D. A. Armitage, M. N. Hughes, A. W. Sinden, *Journal of Chemical Education* **1973**, *50*, 434.

[36] L. Zepeda-Velazquez, B. Macphail, M. A. Brook, *Polymer Chemistry* **2016**, *7*, 4458.

[37] J.-C. Lai, J.-F. Mei, X.-Y. Jia, C.-H. Li, X.-Z. You, Z. Bao, *Advanced Materials* **2016**, *28*, 8277.

[38] J. Lee, B. B. Jing, L. E. Porath, N. R. Sottos, C. M. Evans, *Macromolecules* **2020**, *53*, 4741.

[39] T. J. Wallin, L.-E. Simonsen, W. Pan, K. Wang, E. Giannelis, R. F. Shepherd, Y. Mengüç, *Nature Communications* **2020**, *11*, 4000.

[40] S. Kim, H. Jeon, S. Shin, S. Park, J. Jegal, S. Y. Hwang, D. X. Oh, J. Park, *Advanced Materials* **2018**, *30*, 1705145.

[41] J. Kang, D. Son, G. N. Wang, Y. Liu, J. Lopez, Y. Kim, J. Y. Oh, T. Katsumata, J. Mun, Y. Lee, L. Jin, J. B. -H. Tok, Z. Bao, *Advanced Materials* **2018**, *30*, 1706846.

[42] M. Tang, P. Zheng, K. Wang, Y. Qin, Y. Jiang, Y. Cheng, Z. Li, L. Wu, *Journal of Materials Chemistry A* **2019**, *7*, 27278.

[43] J. L. Self, C. S. Sample, A. E. Levi, K. Li, R. Xie, J. R. de Alaniz, C. M. Bates, *Journal of the American Chemical Society* **2020**, *142*, 7567.

[44] L.-H. Cai, *Soft Matter* **2020**, *16*, 6259.

[45] Z. Wang, C. Xiang, X. Yao, P. Floch, J. Mendez, Z. Suo, *Proceedings of the National Academy of Sciences* **2019**, *116*, 5967.

[46] C. Chen, Z. Wang, Z. Suo, *Extreme Mechanics Letters* **2017**, *10*, 50.

[47] J. Liu, C. Yang, T. Yin, Z. Wang, S. Qu, Z. Suo, *Journal of the Mechanics and Physics of Solids* **2019**, *133*, 103737.

[48] K. Lee, D. J. Mooney, *Chemical Reviews* **2001**, *101*, 1869.

[49] M. Vatankhah-Varnosfaderani, W. F. M. Daniel, M. H. Everhart, A. A. Pandya, H. Liang, K. Matyjaszewski, A. V. Dobrynin, S. S. Sheiko, *Nature* **2017**, *549*, 497.

[50] J. Zhu, Y. He, L. Kong, Z. He, K. Y. Kang, S. P. Grady, L. Q. Nguyen, D. Chen, Y. Wang, J. Oberholzer, L. Cai, *Adv Funct Mater* **2022**, *32*, 2109004.

[51] R. Bai, Q. Yang, J. Tang, X. P. Morelle, J. Vlassak, Z. Suo, *Extreme Mechanics Letters* **2017**, *15*, 91.

[52] D. J. Fortman, J. P. Brutman, G. X. Hoe, R. L. Snyder, W. R. Dichtel, M. A. Hillmyer, *ACS Sustainable Chemistry & Engineering* **2018**, *6*, 11145.

[53] Q. Shi, K. Yu, X. Kuang, X. Mu, C. K. Dunn, M. L. Dunn, T. Wang, H. J. Qi, *Materials Horizons* **2017**, *4*, 598.

[54] B. B. Jing, C. M. Evans, *Journal of the American Chemical Society* **2019**, *141*, 18932.